



# A note on chaotic vs. stochastic behavior of the high-latitude ionospheric plasma density fluctuations

A. W. Wernik, K. C. Yeh

## ► To cite this version:

A. W. Wernik, K. C. Yeh. A note on chaotic vs. stochastic behavior of the high-latitude ionospheric plasma density fluctuations. *Nonlinear Processes in Geophysics*, 1996, 3 (1), pp.47-57. hal-00301804

**HAL Id: hal-00301804**

**<https://hal.science/hal-00301804>**

Submitted on 18 Jun 2008

**HAL** is a multi-disciplinary open access archive for the deposit and dissemination of scientific research documents, whether they are published or not. The documents may come from teaching and research institutions in France or abroad, or from public or private research centers.

L'archive ouverte pluridisciplinaire **HAL**, est destinée au dépôt et à la diffusion de documents scientifiques de niveau recherche, publiés ou non, émanant des établissements d'enseignement et de recherche français ou étrangers, des laboratoires publics ou privés.

## Errata

### A note on chaotic vs. stochastic behavior of the high-latitude ionospheric plasma density fluctuations

**A.W. Wernik<sup>1</sup> and K.C. Yeh<sup>2</sup>**

<sup>1</sup> Space Research Center, Polish Academy of Sciences, ul. Bartycka 18a, Warsaw, Poland

<sup>2</sup> College of Engineering, National Sun Yat-sen University, Kaohsiung, Taiwan, R.O.C.

Nonlinear Processes in Geophysics (1996) 3: 47

Please note that this is the correct country name of the second author. We kindly ask our readers to excuse the printing error made in the original publication.

Bernd Rauchalles, Editorial Office

# A note on chaotic vs. stochastic behavior of the high-latitude ionospheric plasma density fluctuations

A. W. Wernik<sup>1</sup> and K. C. Yeh<sup>2</sup>

<sup>1</sup> Space Research Center, Polish Academy of Sciences, ul. Bartycka 18a, Warsaw, Poland

<sup>2</sup> College of Engineering, National Sun Yat-sen University, Kaohsiung, Taiwan, P.R. China

Received 11 July 1995 - Accepted 20 November 1995 - Communicated by E. Marsch

**Abstract.** Four data sets of density fluctuations measured in situ by the Dynamics Explorer (DE 2) were analyzed in an attempt to study chaotic nature of the high-latitude turbulence and, in this way to complement the conventional spectral analysis. It has been found that the probability distribution function of density differences is far from Gaussian and similar to that observed in the intermittent fluid or MHD turbulence. This indicates that ionospheric density fluctuations are not stochastic but coherent to some extent. Wayland's and surrogate data tests for determinism in a time series of density data allowed us to differentiate between regions of intense shear and moderate shear. We observe that in the region of strong field aligned currents (FAC) and intense shear, or along the convection in the collisional regime, ionospheric turbulence behaves like a random noise with non-Gaussian statistics implying that the underlying physical process is nondeterministic. On the other hand, when FACs are weak, and shear is moderate or observations made in the inertial regime the turbulence is chaotic. The attractor dimension is lowest (1.9) for "old" convected irregularities. The dimension 3.2 is found for turbulence in the inertial regime and considerably smaller (2.4) in the collisional regime. It is suggested that a high dimension in the inertial regime may be caused by a complicated velocity structure in the shear instability region.

## 1 Introduction

Plasmas in the high-latitude F region ionosphere are highly irregular over a broad range of scale sizes from hundreds of kilometers to centimeters (e.g. Tsunoda, 1988; Kelley, 1989). Several mechanisms have been suggested for the production of irregularities: particle precipitation from the magnetosphere, plasma instabilities, turbulent mixing, and neutral atmosphere dynamics. The relative importance of each mechanism apparently depends on the scale size and

location in the magnetic latitude-local magnetic time coordinates. It is believed that for scale sizes between tens of kilometers and tens of meters plasma instabilities are a dominant source of irregularities. This is reasonable since a variety of free energy sources needed to drive instabilities exist in the high-latitude ionosphere; they are for example density gradients, velocity shears, and currents. Due to the magnetic field geometry at high latitudes, and large parallel conductivity, the strong coupling between the ionosphere and magnetosphere plays an important role on irregularity generation and its subsequent convection. Plasma instabilities in the ionosphere have been extensively discussed in the linear regime, but a full understanding of turbulence and its comparison with experiments is possible only for nonlinear models.

Keskinen and Ossakow (1982) have proposed the  $\mathbf{E} \times \mathbf{B}$  instability as a source of high-latitude irregularities. Numerical 2D simulations of the nonlinear evolution of the  $\mathbf{E} \times \mathbf{B}$  instability with the ionosphere-magnetosphere coupling effect included (Mitchell et al., 1985; Huba et al., 1988) showed a difference in the evolution of irregularities between the inertial (strong ionosphere-magnetosphere coupling) and collisional (weak coupling) regimes. Recently, Keskinen and Huba (1990) introduced a scale size dependent coupling into simulations and found that for scale sizes of a few kilometers interchange modes can be characterized as neither purely inertial nor purely collisional.

Similar simulations (Keskinen et al., 1988; Huba et al., 1988) have been made for the Kelvin-Helmholtz (K-H) instability due to the velocity shear flows (Kintner, 1976; Kintner and Seyler, 1985). The nature of K-H instability is different from that of the  $\mathbf{E} \times \mathbf{B}$  instability, since it is driven by the ion inertia, rather than ion Pedersen currents. Thus it is expected that the Kelvin-Helmholtz instability will operate in the topside F region and in the magnetosphere. Simulations show that collisions suppress large scale structures resulting in shallower spectra than that in the

inertial regime.

The main characteristic obtained in simulations is the spatial power spectrum of the electric field ( $\delta E$ ) and plasma density fluctuations ( $\delta n/n$ ) which can be directly compared with observations. Experimentally it has been found that spectra can be represented by a power-law form  $k^{-p}$  where the spectral index  $p$  is usually slightly different in the two orthogonal directions perpendicular to the magnetic field. Practically, the density spectra for the K-H instability are indistinguishable from the  $E \times B$  instability spectra, thus measurements of density spectra alone will not help in identifying the source of observed turbulence. For the K-H instability the electric field spectra are evidently steeper than density spectra, while for the  $E \times B$  instability spectral indices of  $\delta E$  and  $\delta n/n$  are very close.

Simultaneous density and electric field in situ measurements at high latitudes are discussed in details by Basu et al. (1988, 1990). It was found that in the moderate shear regions the spectra of  $\delta E$  and  $\delta n/n$  in the direction of velocity shear agree with simulations. The same conclusion can be reached for auroral "blobs" and polar cap "patches" believed to be dominated by the  $E \times B$  instability. A dramatic difference has been found in  $\delta E$  which was an order of magnitude larger in the velocity shear regions than in the  $E \times B$  regions for the same levels of density fluctuations.

In a recent paper Heppner et al. (1993) analyzed a large data base of spectra and intensities of electric field as measured by AC spectrometers on board of DE-2 satellite. It is proposed that the averaged intensities and spectral characteristics represent superimposed contributions from: (1) an omnipresent 4 – 512 Hz signal from 2000 – 15 m spatial irregularities with an average power law spectral index  $p = 1.9 \pm 0.2$ , (2) intermittent signals from locally generated shear Alfvén waves having maximum power at frequencies  $< 4$  Hz and averaged  $p \leq 2.8$  extending only to the oxygen ion cyclotron frequency, and (3) the spatial irregularity modulations of both locally and remotely generated Alfvén waves.

An interesting discussion of the interchange instability in the context of chaotic system has been given by Huba et al. (1985) and Hassam et al. (1986). Huba et al. have shown that if only three modes are considered then the system can exhibit a strange attractor in the inertial regime, but not in the collisional regime. However, in a many-mode system, even in the inertial regime, large scale convective cells do not exhibit chaotic behavior (Hassam et al., 1986).

The aim of this paper is to extend the data analysis beyond the spectrum estimation and the phenomenological description of ionospheric irregularities. Plasma density data as measured in situ most often show a lack of periodic or quasi-periodic oscillations, and have a noisy, intermittent character apparently not associated with the instrumental errors. Such a complicated pattern is characteristic of the stochastic or chaotic nonlinear dynamical systems. It is known (Eckmann and Ruelle, 1985; Biskamp, 1993)

that whenever the physical system is nonlinear the classical methods (e.g. the spectral analysis) alone are not adequate to describe it. New statistical techniques are required. Among those one can name the higher-order structure functions, fractal and multifractal analysis, multispectral analysis, etc. In this paper we first discuss the probability distribution function of density fluctuations. We show that the statistics of density fluctuations is non-Gaussian. Such a behavior is usually conceived as resulting from a nonlinear deterministic, chaotic, process. Whether really ionospheric plasma turbulence represents a deterministic chaos, or non-Gaussian correlated noise can be judged using tests especially designed for this purpose. Deterministic chaos implies that the dynamics can be described by only a few degrees of freedom, which can be viewed as the dimension of a state space (in mathematics the "state space" is often called the "phase space") in which the system evolves forming a fractal set - strange attractor. We analyzed the density data along this line in an attempt to find if the ionospheric turbulence represents a chaotic system and if some characteristics of the system can be used to discriminate between various geophysical situations.

It should be noted that in the following discussion we assume "frozen in turbulence", which is valid only if the satellite velocity relative to the plasma is much larger than the turbulent velocity. While this is almost always true in the case of satellite measurements it may be not satisfied in the intense velocity shear regions (Basu et al., 1988; Kintner and Seyler, 1985). Additional complications in converting measured temporal fluctuations into spatial variations arise if plasma density irregularities are anisotropic providing some ambiguity in the interpretation of data.

## 2 Data sets

Four data sets of plasma density fluctuations observed by the DE 2 satellite using the retarding potential analyzer (RPA) (Hanson et al., 1981) are discussed. The RPA provided the ion density values at a rate of 64 Hz or approximately every 120 m along the satellite path. The meaningful nonlinear statistical analysis requires long data sets. As a rational compromise between this demand and the need for conservation of geophysical parameters determining the state of the ionosphere data sets of 4096 points, or 64 seconds, long have been chosen. The parameters of the data sets are given in Table 1. The data sets have been selected to cover various geophysical situations. For the first two data sets the orbit plane is orthogonal to the direction of convection. The convection is predominantly sunward for the data set 1, and fluctuating for set 2 (c.f. Figs. 1 and 8 of Basu et al. (1990) where also a more detailed description of orbits 4429 and 3223 can be found. The orbit 1189 is described in Basu et al. (1988)). These two data sets are considered as examples of structures

Table 1. Parameters of data sets

Set #	Orbit #	UT (hh:mm:ss)	Geographic latitude (deg)	Geographic longitude (deg)	Invariant latitude (deg)	Local magnetic time (hr)	Altitude (km)	Average concentration ( $m^{-3}$ )	Remarks
1	4429	21:49:20 – 21:50:24	-54.05 – -58.28	128.49 – 128.23	68.85 – 73.40	7.22 – 7.32	350.15 – 361.98	$5.0 \cdot 10^{10}$	Across convection. Convection predominantly sunward. Large FAC and intense shear. "Collisional" regime.
2	4429	21:50:40 – 21:51:44	-59.34 – -63.56	128.17 – 127.91	74.52 – 78.97	7.35 – 7.52	365.05 – 377.80	$4.3 \cdot 10^{10}$	Across convection. Convection is changing direction. Small FAC and moderate shear. "Collisional" regime.
3	3223	03:38:55 – 03:39:59	63.23 – 67.33	-59.99 – -60.25	72.82 – 76.51	23.84 – 23.98	481.79 – 465.14	$3.9 \cdot 10^{11}$	Along anti-sunward convection. "Old" irregularities.
4	1189	22:57:08 – 22:58:12	81.59 – 85.20	145.22 – 145.04	75.58 – 78.67	7.42 – 7.14	933.25 – 939.24	$2.7 \cdot 10^{10}$	"Inertial" regime. Moderate shear.

across the convection. The main difference between these two sets is in the strength of the field aligned currents (FAC), being as large as  $40 \mu A m^{-2}$  for set 1, and low ( $\sim 1 \mu A m^{-2}$ ) for set 2 (Basu et al., 1988). Our data set 2 does not coincide exactly with the region identified by Basu et al. (1988) as the medium velocity shear region ( $S_M$  in Basu et al. notation), but the pattern of horizontal drift is similar (Fig. 5 of Basu et al.) thus it is reasonable to assume that set 2 falls into this category of shears. Set 1 encompasses the region of intense velocity shear ( $S_I$ ). For comparison a data set 3 has been chosen. In this case the antisunward convection coincides fairly well with the orbital plane of the satellite.

The satellite altitude for the first two data sets was around the F region peak. Set 4 was observed in the top-side ionosphere. If the local parameters are considered, then the first two data sets correspond to the collisional regime and a set 4 to the inertial regime. For this reason we will call the first two sets "collisional", and the last one "inertial".

Figure 1 shows the relative plasma density fluctuations  $\delta n/n$  for all four analyzed data sets. Time is given in seconds relative to the instant of the first data point as given in Table 1. The relative density fluctuations have been computed by subtracting a linear trend from each original data point and dividing by the background density at this point. The standard deviations  $\sigma_{\delta n/n}$  are given in Table 2. The fluctuation pattern is similar for all data sets, except set 3 which looks smoother and is dominated by large scale variations.

In Fig. 2 the power spectra are computed using Welch

Table 2. Derived statistical parameters

Set #	$\sigma_{\delta n/n}$	Skewness	Kurtosis	Spectral slope	Attractor dimension	
					$d_o$	$d_s$
1	0.23	-0.06	9.0	1.89	2.2	2.9
2	0.16	-0.31	12.4	1.73	2.4	3.7
3	0.09	-0.16	9.6	1.51	1.9	2.4
4	0.06	0.05	7.2	1.70	3.2	4.4

method (Welch, 1967) with 2048 points in FFT. Spectra are normalized to the variance and plotted using the dB ordinate scale and logarithmic frequency scale. All spectra exhibit a familiar power-law behavior  $f^{-p}$ . The spectral index  $p$  has been calculated over the frequency range from 0.5 to 10 Hz and is listed in Table 2. All spectra, except set 3, are well characterized by a single slope in this frequency range. Spectrum for the data set 3 shows three slopes, namely 1.76, 1.26, and 1.86 for 0.5 – 1.2, 1.2 – 10, and 10 – 30 Hz, respectively. The domination of large scale fluctuations appears on the spectrum as a relatively large spectral power at frequencies less than 0.3 Hz. A detailed discussion of the plasma density and electric field spectra can be found in Basu et al. (1988, 1990).

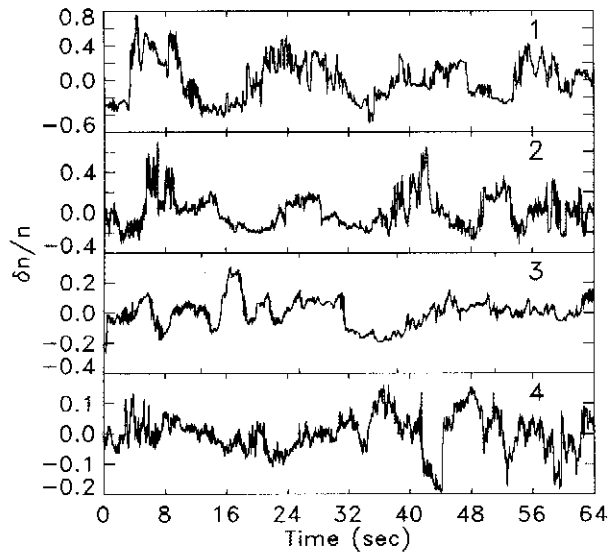


Fig. 1. Relative plasma density fluctuations from RPA for four analyzed data sets.

### 3 Probability distribution function

In general any signal  $x(t)$  generated by a linear or Gaussian process has a Gaussian probability distribution function (pdf) for the differences  $\Delta x(\delta t) = x(t+\delta t) - x(t)$ . The multivariate Gaussian probability distribution function of random fluid variables is a basic assumption in the classical fluid or MHD turbulence (Biskamp, 1993). well as simulations (Vincent and Meneguzzi, 1991) show, however, that this is true only for large time lag  $\delta t$ . For a small lag  $\delta t$ , the distributions differ significantly from Gaussian, being sharply peaked and narrow at small  $\Delta x(\delta t)$  and broad for large differences. The non-Gaussian behavior of distribution at a small separation is interpreted as evidence for intermittency and dominance of the local deterministic dynamics over random processes. Therefore analysis of probability distribution functions of relative plasma density fluctuations  $\delta n/n$  measured in the ionosphere could provide a first test for nonlinear, and/or deterministic nature of ionospheric turbulence generation processes. In the experimental study of turbulence the velocity field is usually analyzed. However, Basu et al. (1990) have shown that  $\delta n/n$  is proportional to the electric field fluctuations  $\delta E$  (hence velocity fluctuations) both in the velocity shear and polar cap patches regions, thus we should expect that the velocity pdf will be similar to that of the density. Similarity between density and velocity pdf's is evident for solar wind fluctuations (Marsch and Tu, 1994).

Probability distribution functions of the differences  $\Delta n(\delta t)$  of relative density fluctuations normalized to zero mean are shown in Fig. 3 for the data sets considered. The time lag  $\delta t$  is one sampling time or 0.015625 s. For comparison the Gaussian (dashed line) and Laplace (double-sided exponential) (continuous line) pdf's are also plotted. The parameters of these distributions ( $\sigma$  and  $\beta$  for

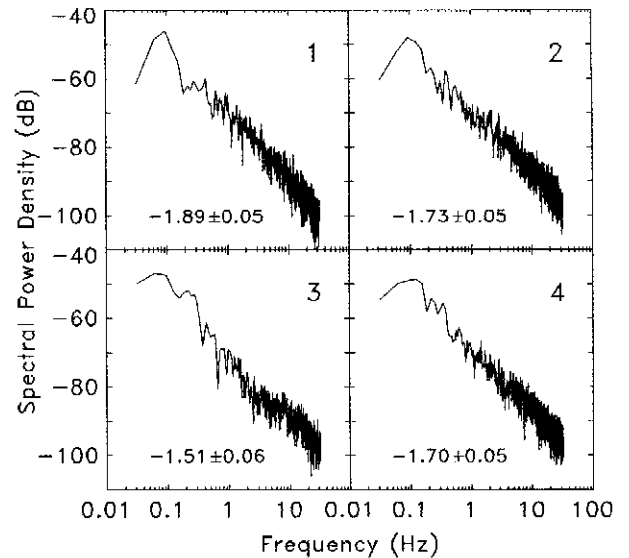


Fig. 2. Power spectra of plasma density fluctuations. Slopes of the spectra, given in Fig., have been calculated over the frequency range 0.5-10 Hz. Note, however, that spectrum 3 has different slopes in different frequency ranges.

the Gaussian and Laplace pdf, respectively) have been calculated from the data. The area under the observed and calculated pdf's is normalized to unity. In all four cases the observed pdf's differ markedly from a Gaussian pdf, since each is more peaked in the central part and curved upwards with an enhanced tail. Except for large fluctuations the distributions are closer to the Laplace pdf. This has been qualitatively confirmed by the  $\chi^2$  test applied to the data. Such behavior of pdf's is a direct evidence of intermittency in ionospheric plasma turbulence. The turbulence is intermittent whenever the energy transfer or dissipation rate is fluctuating and nonuniformly distributed in space, and is typical in fully developed turbulence.

Table 2 lists skewness and kurtosis of the observed pdf's with  $\delta t = 0.015625$  s. To discuss the significance of obtained values note that the standard deviation of skewness for the Gaussian distribution is  $\sqrt{6/N} = 0.04$ , where  $N$  is the number of points in the data set. The skewness is considered significant if it is several times larger than this. Thus only sets 2 and 3 have a notable negative skewness indicating that the distribution has an asymmetric tail the extending towards negative differences. In all four cases kurtosis is larger than 3 showing that distributions are more sharply peaked than the Laplace pdf.

In Fig. 4 an example of pdf's for two time lags is given. A similar picture emerges for other data sets. One can notice that for a large lag the observed pdf becomes Gaussian, again in agreement with experiments on fluid turbulence and simulations.

The conclusion of this section is that ionospheric density fluctuations have the probability distribution function similar to that observed in the intermittent fluid turbulence and MHD turbulence.

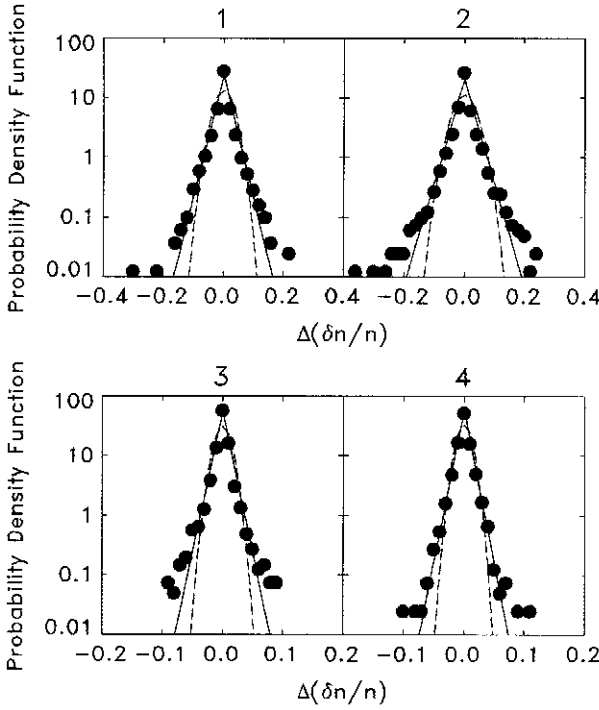


**Fig. 3.** Observed probability density function (full circles) of differenced plasma density fluctuations with superimposed Gaussian (dashed line) and Laplace (continuous lines) distributions with the distribution parameters derived from data. The time lag is one sample time.

#### 4 Tests for determinism

Non-Gaussian probability distribution function of plasma density fluctuation is a convincing argument for the non-linear nature of dynamical processes leading to ionospheric plasma turbulence. However, additional tests are needed to answer the question whether the observed variability of plasma density is due to internal deterministic, low dimensional, dynamics or represents just a noise with non-Gaussian pdf. In fact a variety of tests for determinism in experimental data exist and unfortunately none is fully reliable. The problem is that experimental data are often noisy and too short. Additional difficulties are encountered when data are dominated by the colored noise with power-law power spectra (Osborne and Provenzale, 1989; Theiler, 1991). Nevertheless, data must be tested for determinism since otherwise the derived correlation dimension or Lyapunov exponent might indicate chaos where there is none. Such examples are abundant, and they also appear in space physics. Thus before proceeding further we perform additional tests for determinism in the ionospheric plasma density data.

Two tests are applied: (1) Wayland's test (Wayland et al., 1993), (2) surrogate data test (Theiler et al., 1992). The first test makes use of the "state space continuity" in deterministic systems, i.e. tangents to the trajectory in a given region of state space have similar orientation. From a time series  $x(t_j)$ , in our case a series of  $\delta n/n$  values, the

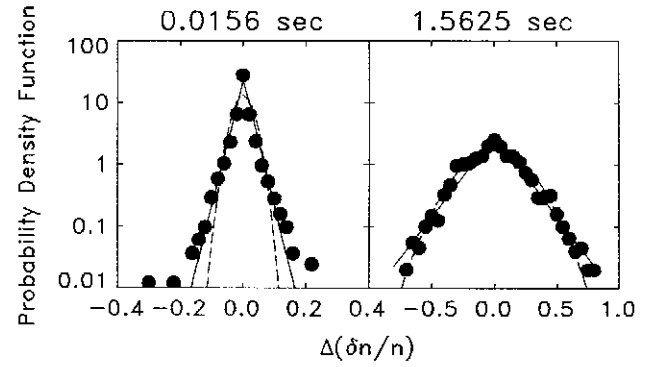


**Fig. 4.** Probability density function of differenced plasma density fluctuations for two time lags (full circles). Dashed and continuous lines are Gaussian and Laplace distributions, respectively.

sequence of  $m$ -dimensional vectors is formed

$$\mathbf{X}_j = (x(t_j), x(t_j + \tau), \dots, x(t_j + (m-1)\tau)) \quad (1)$$

The time delay  $\tau$  is chosen according to a normal procedure used in the reconstruction of the state space (Section 5). Let  $\mathbf{X}_0$  be a fixed, but otherwise arbitrary, vector, and let us choose its  $k$  nearest neighbors  $\mathbf{X}_i$ . Form the images  $\mathbf{Y}_i$  of these vectors ( $\mathbf{Y}_i \equiv \mathbf{Y}(t_i) = \mathbf{X}(t_i + \tau)$ ) and the translation vectors  $\mathbf{v}_i = \mathbf{Y}_i - \mathbf{X}_i$ . If the data are deterministic we expect the translation vectors to be nearly equal. To quantify this notion, let compute the translation error

$$e_t = \frac{1}{k+1} \sum_{j=0}^k \frac{\|\mathbf{v}_j - \langle \mathbf{v} \rangle\|^2}{\|\langle \mathbf{v} \rangle\|^2} \quad (2)$$

where  $\langle \mathbf{v} \rangle = \frac{1}{k+1} \sum_{j=0}^k \mathbf{v}_j$  and  $\|\cdot\|$  denotes the Euclidean

norm. Division by the length of the vector  $\langle \mathbf{v} \rangle$  makes the translation error independent of the overall scaling. If the system is deterministic the translation error will be small. In real computations the translation error has been calculated for many (usually 200) randomly chosen centers and averaged. The number of neighbors  $k$  has been taken to be 4 and the value of embedding dimension  $m$  has ranged from 2 to 9. Results of computations are presented in Fig. 5 for all four data sets (stars and continuous lines) and for comparison, in the bottom panel, for the Lorenz attractor (squares) and white Gaussian noise (diamonds). One can see that the white Gaussian noise gives the translation error close to 1. The translation error for density is small and close to, or even smaller than that for the Lorenz attractor. This implies that we are dealing with a deterministic system. But this is still not fully convincing conclusion because random data with the same power spectrum as the original data may also lead to a small translation error. Yet another test using the surrogate data should be applied.

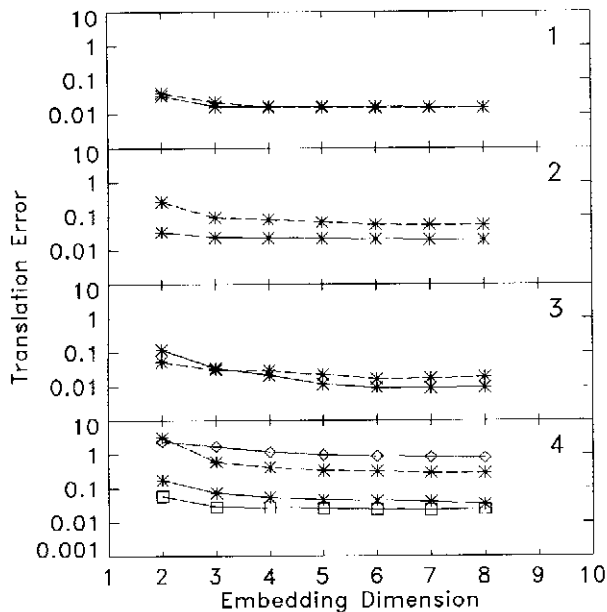


Fig. 5. Translation error versus embedding dimension. Continuous and dashed lines with stars are original and surrogate data, respectively. Results of computations for the white Gaussian noise (diamonds) and Lorenz attractor (squares) are also shown in the bottom panel.

The surrogate data series has been generated from the original data set using the amplitude adjusted Fourier transform (AAFT) algorithm (for details see Theiler et al., 1992). It gives a time series which has the same power spectrum and amplitude distribution as the original, however any coherency which may be present in the original data is destroyed. The AAFT algorithm has been used instead of the simpler randomization of the Fourier phase because, as we have seen in the previous section, the data have apparently non-Gaussian distribution. The surrogate data set generated with AAFT can be considered as resulting from a monotonic nonlinear transformation of a linear random Gaussian process. This is our null hypothesis against which observations are tested. As a discriminating statistics (Theiler et al., 1992), which is a number quantifying the departure of observations from the null hypothesis, we will take the translation error and, in the next section, the correlation dimension.

The translation error as calculated for surrogate data is plotted in Fig. 5 in dashed lines. One can see that for sets 1 and 3 the translation error is similar to that for the original data which suggests that the original data behave like the non-Gaussian random noise. The surrogate data for sets 2 and 4 give the translation errors larger than that for the original data. To evaluate the significance of the difference we apply a Student *t*-test and calculate the probability when the translation error for the original data and that for the surrogate data are equal by chance. For sets considered these probabilities are: 0.31, 0.02, 0.84, 0.09, respectively. Thus we conclude that in the region of strong FAC, and intense shear, or along the convection in

the “collisional” regime, ionospheric turbulence behaves like a stochastic random noise with non-Gaussian statistics. On the other hand, when FAC are weak, and shear is moderate or observations made in the “inertial” regime the turbulence is chaotic.

## 5 Correlation dimension

The correlation dimension is the most widely used parameter to characterize the complexity of chaotic behavior of a dynamical system. It counts the number of degrees of freedom of a system, or the number of independent variables needed to describe the physical process. The popularity of the correlation dimension stems from relative ease with which it can be calculated. But in fact, the correlation dimension is only one from a whole set (spectrum) of dimensions which is normally required to fully describe a system. In this paper, however, we will be concerned only with the correlation dimension.

Calculation of the correlation dimension is relatively simple and many algorithms in existence can be used. However, the important question about reliability and accuracy of these methods remains open in spite of long-lasting discussion among specialists (Mayer-Kress, 1989; Theiler, 1990; Ott et al., 1994). Most algorithms require the following steps: (1) reconstruction of the system trajectory in the *m*-dimensional state space, (2) calculation of the dimension, (3) verification of results.

One of the most remarkable findings of the chaos theory is that the system trajectory (attractor) can be reconstructed from a time series of one state variable (e.g., temperature, plasma density, AL magnetic index) (Packard et al., 1980). The impact of this discovery on the practical implementation of chaos theory is tremendous: even the most complicated systems can be analyzed based on the knowledge of only one state variable. The reconstructed trajectory is not exactly the same as the original one, but it reproduces many topological features, and in particular has the same dimension as the original (Takens, 1981). This, so called time-delay coordinates method, has already been used in Section 4.

For a long time series of the noise-free, stationary data arbitrary time delay  $\tau$  can be taken. In practice, however, the choice of  $\tau$  is critical (Havstad and Ehlers, 1989; Theiler, 1990) and should assure the independence of coordinates of the vector  $X_j$ . Fraser and Swinney (1986) have presented a method to find the optimum value of  $\tau$  by calculating the first minimum of the mutual information. The mutual information measures the dependence of two variables in a more general way than the autocorrelation function. However, the method is complicated and requires very large data sets unless the dimension is low. Therefore in our calculations we have chosen  $\tau$  equal to the correlation time, defined as a time of the first zero of autocorrelation function.

The correlation dimension is calculated using a com-



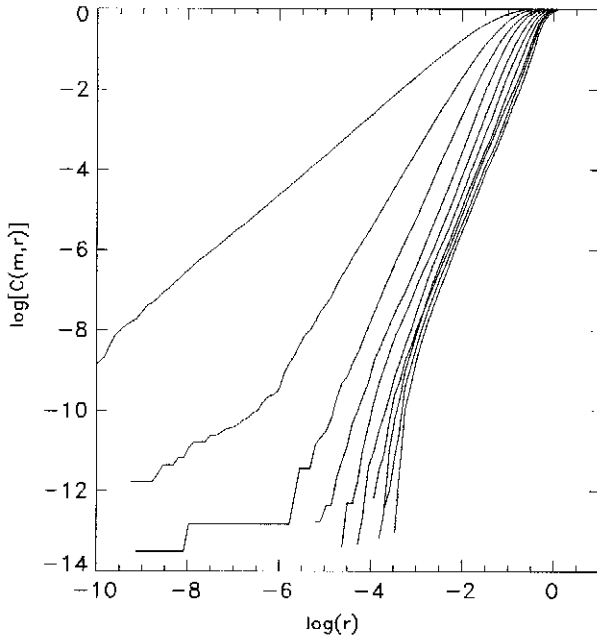


Fig. 6. Log-log plots of the correlation integral  $C(m, r)$  vs.  $r$  for data set 4 ( $m = 1 \dots 10$  from top to bottom).

mon correlation integral method (Grassberger and Procaccia, 1983). The correlation integral  $C(m, r)$  is defined as follows:

$$C(m, r) = \frac{1}{N_{ref}(N-1)} \sum_{i=1}^{N_{ref}} \sum_{\substack{j=1 \\ j \neq i}}^N H(r - |X_i - X_j|) \quad (3)$$

where  $H(z)$  is the Heaviside step function:  $H(z)$  is zero for  $z < 0$  and one for  $z > 0$ .  $|X_i - X_j|$  is a distance between points  $X_i$  and  $X_j$  in the  $m$ -dimensional state space.  $N_{ref}$  is the number of reference vectors. In most algorithms this is equal to a total number of vectors  $N$ . However, we have found, in agreement with Holzfuss and Mayer-Kress (1989), that significantly smaller number of reference vectors is sufficient and took  $N_{ref} = 200$ . This substantially saves the amount of computer time and memory.

For small distances  $r$  the correlation integral scales as:

$$\lim_{r \rightarrow 0} C(m, r) \propto r^{v_m} \quad (4)$$

where  $v_m$  is the correlation dimension at the embedding dimension  $m$ . If the correlation dimension is computed for a number of embedding dimensions then, for sufficiently large  $m$ ,  $v_m$  should be independent of  $m$ . This constant value of  $v_m$  is a measure (lower bound) of the attractor dimension  $d$ .

It is generally accepted that the dimension estimate is more reliable for longer data sets. However, specialists in chaotic system analysis have not reached a consensus as what is the smallest useful data set. For instance, Eckmann

and Ruelle (1992) claim that if the dimension is determined from  $N$  vectors, then one should not believe a dimension estimate that is not well below  $2 \log_{10} N$ . When the number of reference vectors  $N_{ref}$  is not equal to the total number of vectors  $N$  this result should be slightly modified and assumes a form  $\log_{10}(N \cdot N_{ref})$ . From a series of  $N_d$  data points  $N_d - m \cdot \tau + 1$  vectors can be constructed. Our data sets are  $N_d = 4096$  points long which for the longest observed correlation time  $\tau = 270$  points and  $m = 10$  gives  $N = 1395$  vectors. With  $N_{ref} = 200$  the upper limit to the dimension  $d$  is 5.4. Roberts (1991) argues that  $N > 10^d$  is required. It seems that this is too pessimistic an estimate. Havstad and Ehlers (1989) have shown by numerical computations that the independence of vectors in the state space is essential and, if satisfied, even a small data set would suffice for reliable reconstruction of the attractor and its dimension, provided all measures are taken to correct for short data set effects.

The correlation dimension  $v_m$  has been computed using two methods: (1) by a linear least squares fitting to the  $\log C$  vs.  $\log r$  plot, (2) by calculating a local slope  $d(\log C)/d(\log r)$ . As an example, in Fig. 6 we present  $\log C$  vs.  $\log r$  plot for the data set 4 and  $m$  ranging from 1 to 10. The behavior of curves is typical and its discussion can be found in the literature (e.g. Havstad and Ehlers, 1988; Theiler, 1990, 1991). By definition (4),  $v_m$  is the correlation dimension only in the limit of small  $r$ . However, at small  $r$  ( $\log r < -3$  in our example) the instrumental and measurement noise is dominant. Since random noise fills all dimensions of state space, the slope in this region approaches the value of embedding dimension. Often experimentalists are tempted to improve the data quality by filtering out the noise, but this is not recommended since, as shown by Badii et al. (1988), low-pass filtering increases the correlation dimension. At large  $r$  ( $\log r > -0.8$  in our example) the slope increases. The reason for this is that when  $r$  is large we approach the edge of the attractor where scaling of  $C(m, r)$  is different (Theiler, 1990). The algorithm used for the least squares fitting has a provision for automatic search for the scaling region of  $\log r$  for which  $v_m$  is calculated (Wernik and Yeh, 1994). It gives the correlation dimensions agreeing, within errors, with that obtained by the local slope method.

In the local slope method a derivative  $d(\log C)/d(\log r)$  is calculated numerically. Next, a plot  $d(\log C)/d(\log r)$  vs.  $\log r$  is constructed for each embedding dimension. If the scaling region exists, then for sufficiently large  $m$  the curve would exhibit a plateau at  $d(\log C)/d(\log r) \sim v_m$ . Graphs of slope versus  $\log r$  are shown in Fig. 7 for the original and surrogate data of set 4. The embedding dimension changes from  $m = 1$  to 10. Three distinct regions can be distinguished in the original data plot: the noise region at small  $r$ , plateau or scaling region ( $-2.8 < \log r < -0.8$ ), and "edge effect" region at large  $r$ . To get the correlation dimension the local slopes have been averaged within the scaling region for each embedding dimension. For the surrogate data the scaling region is practically non-

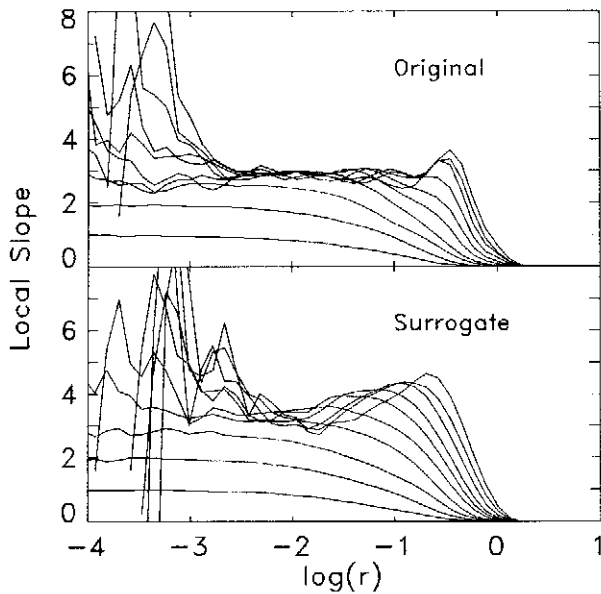


Fig. 7. Plot of slope  $d(\log C)/d(\log r)$  vs.  $\log r$  for the original and surrogate data sets 4. Different curves correspond to different embedding dimensions.

existent. Nevertheless, the correlation dimension has been calculated using the same scaling region as estimated for the original data.

In Fig. 8 the correlation dimension  $\nu_m$  is plotted versus embedding dimension  $m$  for all four pairs of the original (crosses) and surrogate (stars) data sets. The attractor dimension  $d$  is calculated as a mean of  $\nu_m$  for embedding dimensions for which  $\nu_m$  levels off. Theoretically the limiting value of  $m$  should be close to  $\text{int}(2d+1)$  (Takens, 1981), but in practice asymptotic behavior is reached at a smaller  $m$ . Final values of attractor dimensions are given in Table 2 for both the original ( $d_o$ ) and surrogate ( $d_s$ ) data. To assess the statistical significance of the difference between  $d_o$  and  $d_s$  the Student's t-test is applied to  $\nu_m$  from which the attractor dimension is calculated. In all cases the difference is significant at level less than  $10^{-3}$  which means that the null hypothesis should be rejected. In other words the original data do not portray non-Gaussian noise. This seems to contradict the conclusion of previous Section where it has been found that only sets 2 and 4 represent chaotic systems. However, closer inspection of Fig. 7 reveals that original and surrogate correlation dimensions for sets 1 and 3 are, slightly but evidently, closer to each other than those for sets 2 and 4. Therefore we claim that sets 1 and 3 indeed conform to the null hypothesis (although on a very low probability level), while sets 2 and 4 do not. This leads us to the conclusion that the surrogate data test for chaoticity in plasma density data, with the correlation dimension as a discriminating statistical parameter, gives result in agreement with the Wayland's test.

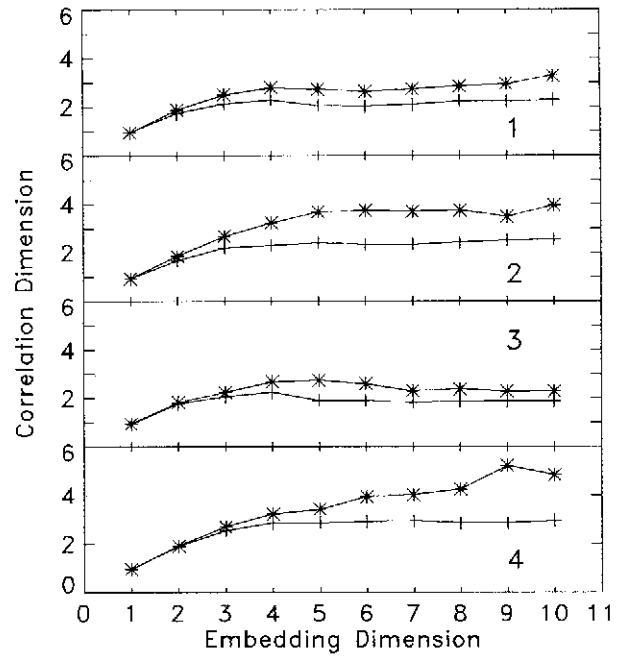


Fig. 8. Plot of the correlation dimension vs. embedding dimension for original (crosses) and surrogate (stars) data for each of the analyzed sets.

## 6 Discussion and conclusions

We have analyzed four data sets of fluctuating plasma density measured in various geophysical situations in the high-latitude ionospheric F region. In all cases the probability distribution function of density differences  $\Delta n(\delta t)$  is significantly different from Gaussian for relatively short delays  $\delta t$ , being sharply peaked for small  $\Delta n$ , reduced for intermediate, and enhanced for large  $\Delta n$ . Distribution approaches Gaussian for large delays. This behavior is similar to that observed in the laboratory and simulations of fluid and MHD turbulence. Distributions resemble recent observations of solar wind density and velocity pdf's (Marsch and Tu, 1994). This result means that the statistics of  $\delta n/n$  is dominated by sparsely distributed large scale fluctuations, a direct evidence of temporal intermittency. The temporal intermittency can be identified with the spatial intermittency for "frozen in" turbulence. One should keep in mind, however, that the "frozen in" assumption may be violated in the regions of large velocity shears. Different statistical properties of  $\delta n/n$  at different scales indicate that density fluctuations have a multifractal character.

Intermittency is discussed in various models of fluid and MHD turbulence (c.f. Paladin and Vulpiani, 1987; Biskamp, 1993). In fact, it is intermittency which led Obukhov(1962) and Kolmogorov (1962) to the lognormal model of energy dissipation in turbulence. Recently, She and Orszag (1991) (see also Biskamp (1993)) derived the probability distribution function based on the argument that at small scales only small amplitude eddies undergo

the Kolmogorov local cascade, while large amplitude vortices suffer self-distortion and stretching. The simplest form of their probability distribution function for a turbulent velocity  $\delta v$  is then given by:

$$P(\delta v) \propto \exp(-c|\delta v|^{1+h}) \quad (5)$$

For  $h = 0$   $P(\delta v)$  reduces to the Laplace distribution with  $c = 1/\beta$ . Although  $P(\delta v)$  has been derived for velocity fluctuations it should still hold for relative density fluctuations, thus we tried to fit the parameter  $h$  to the observed pdf's with  $\delta t = 0.015625$  sec, and found that it is negative and its absolute value is relatively small, less than 0.13. This means that at small scales the large amplitude eddies undergo rather weak stretching. It should be noted, however, that the random  $\beta$  - model of turbulence (Novikov and Stewart, 1964), which does not assume any stretching of large amplitude eddies, also gives pdf (Benzi et al., 1991) which can fit our observations. Thus it is risky to make any firm conclusions about the model of turbulence based just on the observed probability distribution function.

Intermittancy in the ionospheric plasma density means that there is an excess energy in large scale structures. Consequently, spectra are steeper than that for a homogeneous turbulence. In this context we note that Kintner and Seyler (1985), implicitly assuming homogeneity of turbulence, have estimated the spectral indices for density and electric field in the  $\mathbf{E} \times \mathbf{B}$  and K-H instabilities which are consistently smaller than those derived from nonlinear simulations (Mitchell et al., 1985; Keskinen et al., 1988; Keskinen and Huba, 1990).

Non-Gaussian statistics of density fluctuations implies that the turbulence is either a nonlinear, chaotic process, or represent a non-Gaussian noise. Wayland's and surrogate data tests show that in the regions of weak field-aligned currents and moderate shear (data set 2) and in the topside ionosphere, in the "inertial" regime (set 4), the turbulence is chaotic. On the other hand, in the region of strong FAC and intense shear (set 1), and along the convection (set 3), ionospheric turbulence behaves like a noise. Basu et al. (1988) have found that the density spectral indices  $p$  in the moderate and intense shear regions are practically the same. On the other hand, electric field spectral indices differ substantially. They have found that the moderate shear spectra for both density and electric field agree with simulations of the collisional K-H instability. Results of tests for determinism show that a more sophisticated density data analysis reveals the difference between the moderate and intense shear region turbulence not easily discernible with the simple spectral analysis. Non-deterministic nature of turbulence in intense shears supports the suggestion (Basu et al., 1988) that in these regions multiple generation mechanisms of irregularities could operate.

Set 3 corresponds to the situation when the data are taken along convection. The large scale density gradients

along the orbit are weak, which otherwise would favor the generation of irregularities by the  $\mathbf{E} \times \mathbf{B}$  instability. The flux of precipitating electrons is rather small (c.f. Plate 1 of Basu et al., 1990), and no velocity shears are observed. Therefore it is reasonable to assume that irregularities observed in this set are not locally generated but rather were convected across the polar cap from some remote generation regions. An additional argument for this assumption is given by the spectrum which exhibits a relatively small slope for structures larger than 25 km ( $f < 0.03$  Hz), in agreement with Kelley et al. (1982) who showed that on the transit of the polar cap small scale irregularities are washed out by turbulent diffusion. Apparently, during their lifetime the "old" irregularities are subject to various influences, some deterministic, some stochastic, so that the locally measured turbulent density can not be considered as an autonomous system which is required for chaoticity.

In set 4 no appreciable density gradients are observed and the velocity shear falls into the moderate category (Fig. 14 of Basu et al., 1988). The main difference between this data set and set 2 is the altitude, which is much lower for the later. It is reasonable to assume that set 4 corresponds to the locally inertial, collisionless, regime, and set 2 to the collisional regime. While geophysical conditions and certain characteristics of turbulence are similar for both sets, one should keep in mind that measurements are not simultaneous. Nevertheless, it may be of interest to discuss these sets as examples of two different turbulence regimes: collisional and inertial. Spectral slopes are not very much different, although the inertial regime spectrum (c.f. Fig. 2) seems to be broader at large scales.

Tests for determinism imply deterministic chaos in both cases. The chaotic behavior of fluctuations generated by the interchange instability has been discussed by Huba et al. (1985) and Hassam et al. (1986). Huba et al. have shown that if only three modes are considered then the equations describing the interchange instability reduce to the famous set of Lorenz equations (Lorenz, 1963) which characterize Rayleigh-Benard instability in fluids, and the system can exhibit a strange attractor. However, the ion inertia plays a crucial role in that if it is neglected (as below 450-500 km in the ionosphere) the system fails to be chaotic and a stable convection pattern results. Hassam et al. (1986) claim that in a many-mode system large scale convective cells are not chaotic, even in the inertial regime. The physics of K-H instability is different from that of the  $\mathbf{E} \times \mathbf{B}$  instability, a typical interchange instability, since it is driven by the ion polarization current, rather than ion Pedersen currents. There is no analogy between K-H instability and Rayleigh-Benard instability, that is obvious in the case of  $\mathbf{E} \times \mathbf{B}$  instability. Therefore Huba et al. (1985) results are not applicable to the K-H instability. It is true, however, that any many-mode system, characterized by a large number of degrees of freedom (attractor is high-dimensional), would behave like a random system. The fact that we observe low-dimensional chaos in both

inertial and collisional regimes suggests that only a small number of modes are involved in generating the turbulence in these cases.

The most pronounced difference in the attractor dimension is found between a high value of 3.2 in the inertial regime and a low value of 2.4 in the collisional regimes. Large attractor dimension means that density in the inertial regime is more structured. This contradicts simulations (Keskinen et al., 1988) which show that when collisions are neglected K-H instability forms characteristic large scale vortices and spirals. Only in the collisional regime small scale irregular structures are developed. The model used in simulations assumes a localized single shear interface with a single shear frequency (highest velocity/shear gradient scale length). In reality the satellite traverses several adjacent shear interfaces with different shear frequencies. Vortices generated by each shear interface interact with each other resulting in a structure which is much more complicated than that for a single interface. This effect has a lesser consequence in the weakly collisional K-H instability when the irregular structure is determined by finite Pedersen conductivity and the vortices form only at the initial stage. Therefore a relatively high attractor dimension in the inertial regime indirectly reflects a complicated structure of the velocity in shear region.

Attractor dimensions derived for sets 1 and 3 are very low. We do not have any immediate physical arguments to explain this surprising result. We only note that some kind of self-organizing process must be present in the ionosphere which reduces originally large number of degrees of freedom to just a few degrees of freedom sufficient to describe the turbulent ionosphere. This is a typical problem of synergetics.

The results presented in this paper are based on only four data sets, thus should not be generalized. Yet they show that application of more sophisticated methods of data analysis can provide additional physical insights, especially when the spectral analysis gives ambiguous results. It would be of great interest to apply these methods to results of numerical simulations and compare with observations.

**Acknowledgments.** We wish to thank W.R. Coley for making DE 2 data readily available for this study. We acknowledge useful comments by Su. Basu and Sa. Basu. The joint work was supported by the National Science Foundation grant INT 92-00765. The work by A.W.W. was supported by the Polish Committee on Scientific Research under the grant 2 2150 92 03p/31. This study has been initiated while A.W.W. visited the National Central University on the invitation of the National Research Council of R.O.C. (Taiwan).

## References

- Anselmet, F., Gagne, Y., Hopfinger E.J., and Antonia R.A., High-order velocity structure functions in turbulent shear flows, *J. Fluid Mech.*, **140**, 63-89, 1984.
- Badii, R., Broggi G., Derighetti D., Ravani M., Gilberto S., Politi A., and Rubio M.A., Dimension increase in filtered chaotic signals, *Phys. Rev. Lett.*, **60**, 979-982, 1988.
- Basu, Su., Basu, Sa., MacKenzie, E., Fougere, P.F., Coley, W.R., Maynard, N.C., Winningham, J.D., Sugiura, M., Hanson, W.B., and Hoegy, W.R., Simultaneous density and electric field fluctuation spectra associated with velocity shears in the auroral oval, *J. Geophys. Res.*, **93**, 115-136, 1988.
- Basu, Su., Basu, Sa., MacKenzie, E., Coley, W.R., Sharber, J.R., and Hoegy, W.R., Plasma structuring by the gradient drift instability at high latitudes and comparison with velocity shear driven processes, *J. Geophys. Res.*, **95**, 7799-7818, 1990.
- Benzi, R., Biferle, L., Paladin, G., Vulpiani, A., and Vergalossa, M., Multifractality in the statistics of the velocity gradients in turbulence, *Phys. Rev. Lett.*, **67**, 2299-3002, 1991.
- Biskamp, D., *Nonlinear magnetohydrodynamics*, Cambridge University Press, Cambridge, 1993.
- Eckmann, J.-P. and Ruelle, D., Ergodic theory of chaos and strange attractors, *Rev. Mod. Phys.*, **57**, 617-656, 1985.
- Eckmann, J.-P. and Ruelle, D., Fundamental limitations for estimating dimensions and Lyapunov exponents in dynamical systems, *Physica D*, **56**, 185-187, 1992.
- Fraser, A. and Sinney, H., Independent coordinates for strange attractors from mutual information, *Phys. Rev. A*, **33**, 1134-1140, 1986.
- Grassberger, P. and Procaccia, I., Measuring the strangeness of strange attractors, *Physica D*, **9**, 189-208, 1983.
- Hanson, W.B., Heelis R.A., Power R.A., Lippincott C.R., Zuccaro D.R., Holt B.J., Harmon L.H., and Sanatani, S., The retarding potential analyzer for Dynamics Explorer-B, *Space Sci. Instrum.*, **5**, 503-510, 1981.
- Hassam, A.B., Hall W., Huba J.D., and Keskinen, M.J., Spectral characteristics of interchange turbulence, *J. Geophys. Res.*, **91**, 13513-13522, 1986.
- Havstad, J.W. and Ehlers, C.I., Attractor dimension of nonstationary dynamical systems from small data sets, *Phys. Rev. A*, **39**, 845-853, 1989.
- Heppner, J.P., Liebrecht, M.C., Maynard, N.C., and Pfaff, R.F., High-latitude distributions of plasma waves and spatial irregularities from DE 2 alternating current electric field observations, *J. Geophys. Res.*, **98**, 1629-1652, 1993.
- Holzfluss, J. and Mayer-Kress, G., An approach to error-estimation in the application of dimension algorithms, in: *Dimensions and entropies in chaotic systems* (Ed. G. Mayer-Kress), 114-122, Springer, Berlin (2nd corrected printing), 1989.
- Huba, J.D., Hassam, A.B., Schwartz, I.B., and Keskinen, M.J., Ionospheric turbulence: Interchange instabilities and chaotic fluid behavior, *Geophys. Res. Lett.*, **12**, 65-68, 1985.
- Huba, J.D., Mitchell, H.G., Keskinen, M.J., Fedder, J.A., Satyanarayana, P., and Zalesak, S.T., Simulation of plasma structure evolution in the high-latitude ionosphere, *Radio Sci.*, **23**, 503-512, 1988.
- Kelley, M.C., Vickerey, J.F., Carlson, C.W., and Torbert, R., On the origin and spatial extent of high-latitude F region irregularities, *J. Geophys. Res.*, **87**, 4469-4475, 1982.
- Kelley, M.C., *The Earth ionosphere*, Academic Press, London, 1989.
- Keskinen, M.J. and Ossakow, S.L., Nonlinear evolution of plasma enhancements in the auroral ionosphere, I. Long wavelength irregularities, *J. Geophys. Res.*, **87**, 144-150, 1982.
- Keskinen, M.J., Mitchell, H.G., Fedder, J.A., Satyanarayana, P., Zalesak, S.T., and Huba, J.D., Nonlinear evolution of the Kelvin-Helmholtz instability in the high-latitude ionosphere, *J. Geophys. Res.*, **93**, 137-152, 1988.
- Keskinen, M.J. and Huba, J.D., Nonlinear evolution of high-latitude ionospheric interchange instabilities with scale-size-dependent magnetospheric coupling, *J. Geophys. Res.*, **95**, 15157-15166, 1990.
- Kintner, P.M., Jr., Observations of velocity shear driven plasma turbulence, *J. Geophys. Res.*, **81**, 5114-5122, 1976.

- Kintner, P.M., Jr. and Seyler, C.E., The status of observations and theory of high latitude ionospheric and magnetospheric plasma turbulence, *Space Sci. Rev.*, **41**, 91-129, 1985.
- Kolmogorov, A.N., A refinement of previous hypothesis concerning the local structure of turbulence in a viscous incompressible fluid at high Reynolds number, *J. Fluid Mech.*, **13**, 82-85, 1962.
- Lorenz, E.N., Deterministic nonperiodic flow, *J. Atmos. Sci.*, **20**, 130-141, 1963.
- Marsch, E. and Tu C.Y., Non-Gaussian probability distributions of solar wind fluctuations, *Ann. Geophysicae*, **12**, 1127-1138, 1994.
- Mayer-Kress, G., (Ed.), *Dimensions and entropies in chaotic systems*, Springer, Berlin (2nd corrected printing), 1989.
- Mitchell, H.G., Fedder, J.A., Keskinen, M.J., and Zalesak, S.T., A simulation of high-latitude F-layer instabilities in the presence of magnetosphere-ionosphere coupling, *Geophys. Res. Lett.*, **12**, 283-286, 1985.
- Novikov, E.A. and Stewart, R.W., Intermittancy of turbulence and spectrum of fluctuations in energy dissipation, *Izv. AN SSSR, Ser. Geofiz.*, **3**, 408-413, 1967.
- Obukhov, A.M., Some features of atmospheric turbulence, *J. Fluid Mech.*, **13**, 77-81, 1962.
- Osborne, A.R. and Provenzale, A., Finite correlation dimension for stochastic systems with power-law spectra, *Physica D*, **35**, 357-381, 1989.
- Ott, E., Sauer, T., and Yorke, J.A., (Eds.), *Coping with chaos*, J. Wiley & Sons, New York, 1994.
- Packard, N.H., Crutchfield, J.P., Farmer, J.D., and Shaw, R.S., Geometry from time series, *Phys. Rev. Lett.*, **45**, 712-716, 1980.
- Paladin, G. and Vulpiani, A., Anomalous scaling laws in multifractal objects, *Phys. Rep.*, **156**, 147-225, 1987.
- Roberts, D.A., Is there a strange attractor in the magnetosphere?, *J. Geophys. Res.*, **96**, 16031-16046, 1991.
- She, Z.-S. and Orszag, S.A., Physical model of intermittancy in turbulence: Inertial range non-Gaussian statistics, *Phys. Rev. Lett.*, **66**, 1701-1704, 1991.
- Takens, F., Detecting strange attractors in turbulence, in *Lecture Notes in Mathematics*, **898** (Eds. D.A. Rand and L.S. Young), Springer, Berlin, 366-381, 1981.
- Theiler, J., Estimating the fractal dimension of chaotic time series, *The Lincoln Lab. J.*, **3**, 63-85, 1990.
- Theiler, J., Some comments on the correlation dimension of  $1/f^\alpha$  noise, *Phys. Lett. A*, **155**, 480-493, 1991.
- Theiler, J., Eubank, S., Longlin, A., Galdrikian, B., and Farmer, J.D., Testing for nonlinearity in time series: the method of surrogate data, *Physica D*, **58**, 77-94, 1992.
- Tsunoda, R.T., High-latitude F region irregularities: A review and synthesis, *Rev. Geophys.*, **26**, 719-760, 1988.
- Vincent, A. and Meneguzzi, M., The spatial structure and statistical properties of homogeneous turbulence, *J. Fluid Mech.*, **225**, 1-20, 1991.
- Wayland, R., Bromley, D., Pickett, D., and Passamante, A., Recognizing determinism in a time series, *Phys. Rev. Lett.*, **70**, 580-582, 1993.
- Welch, P.D., The use of fast Fourier transform for the estimation of power spectra: a method based on time averaging over short, modified periodograms, *IEEE Trans. Audio and Electroacoust.*, **AU-15**, 70-73, 1967.
- Wernik, A.W. and Yeh, K.C., Chaotic behavior of ionospheric scintillation: modeling and observations, *Radio Sci.*, **29**, 135-144, 1994.